

Microscopic theory of the coupling of intrinsic Josephson oscillations and phonons

Ch. Preis^a, Ch. Helm^{a,b}, K. Schmalzl^a, Ch. Walter^a, J. Keller^a

^aInstitute of Theoretical Physics, University of Regensburg, D-93040 Regensburg, Germany

^bLos Alamos National Laboratory, Division T-11, M.S. B-262, NM 87545, USA

A microscopic theory for the coupling of intrinsic Josephson oscillations and dispersive phonon branches in layered superconductors is developed. Thereby the effect of phonons on the electronic *c*-axis transport enters through an effective longitudinal dielectric function. This coupling provides an explanation of recently observed subgap resonances in the I_{dc} - V_{dc} -curve of anisotropic cuprate superconductors forming a stack of short Josephson junctions. Due to the finite dispersion these resonances can appear at van-Hove-singularities of both optical and acoustical phonon branches, explaining low-voltage structures in the I-V-characteristic, which are not understood in phonon models without dispersion. In long junctions the dispersion of collective electron-phonon modes parallel to the layers is investigated.

1. INTRODUCTION

The main features of the electronic *c*-axis transport in the high- T_c -superconductors $\text{Tl}_2\text{Ba}_2\text{Ca}_2\text{Cu}_3\text{O}_{10+\delta}$ and $\text{Bi}_2\text{Sr}_2\text{CaCu}_2\text{O}_{8+\delta}$ below the critical temperature T_c can be well understood in the model of a stack of superconducting CuO_2 -layers, which form a onedimensional stack of intrinsic Josephson junctions [1].

One of the few phenomena, which are specific to the *intrinsic* Josephson effect and cannot be seen in arrays of conventional superconductors, is the interaction of the Josephson oscillations and phonons. This has been observed experimentally in the form of resonances in the I_{dc} - V_{dc} -characteristics at low voltages [2–4]. Their main features could already be understood theoretically in the framework of a simple lattice dynamical model of damped local oscillators in the barrier [5].

Despite the clear evidence of the effect a general multi-band theory, in which parameters like the phonon frequencies or the oscillator strength in the dielectric function are specified microscopically, is still missing and shall be presented in the following. This more general formalism is in principle appropriate to include the eigenvalues and eigenvectors of the dynamical matrix as obtained

in *any* microscopic lattice dynamical calculation into the Josephson theory. Qualitative effects of the phonon dispersion are discussed in a simple rigid ion model, e.g. the van-Hove singularity at the upper edge of the acoustical band, which can be detected in the I_{dc} - V_{dc} -curve. Details of the derivation and further results can be found elsewhere [6].

2. THEORY OF PHONON COUPLING

The Josephson effect between the layers n and $n+1$ is described by a RSJ-like equation

$$j = j_c \sin \gamma_n(t) + j_{qp}(E_n(t)) + \epsilon_0 \dot{E}_n^\rho(t),$$

where j is the bias current (density), $j_c \sin \gamma_n(t)$ the supercurrent, $j_{qp}(E_n)$ the quasiparticle current and $\gamma_n(t)$ the gauge-invariant phase difference, which is related to the average electric field $E_n(t)$ in *c*-direction in the barrier: $\hbar \dot{\gamma}_n(t) = 2e d E_n(t)$ (d : thickness of the barrier). In contrast to this, the displacement current density $\epsilon_0 \dot{E}_n^\rho(t)$ does not depend on E_n , but the field $E_n^\rho(t)$ set-up by the conduction-electron charge-fluctuations $\delta\rho_n$ on the layers, which obey the Poisson equation $\delta\rho_n(t) = \epsilon_0(E^\rho(t) - E_{n-1}^\rho(t))$ and the continuity equation $j_n(t) - j_{n-1}(t) = -\delta\dot{\rho}_n(t)$. All quantities are constant along the layers ($q_\parallel = 0$)

as in short junctions.

The crucial point is to determine the (linear) relation between the field

$$E^p(q_z, \omega) = E - E^{\text{ion}} = \epsilon_{\text{ph}}(q_z, \omega)E(q_z, \omega) \quad (1)$$

created by the charge fluctuations alone and the total electric field $E(q_z, \omega)$ due to both electrons and ions. This can be described by the (longitudinal) phonon dielectric function

$$\epsilon_{\text{ph}}^L(q_z, \omega) = \frac{\epsilon_\infty}{1 - \chi(q_z, \omega)}, \quad (2)$$

where the susceptibility (λ : phonon branch)

$$\chi(q_z, \omega) = \sum_{\lambda} \frac{|\Omega(q_z \lambda)|^2}{\omega^2(q_z \lambda) - \omega^2} \quad (3)$$

and the oscillator strength

$$|\Omega(q_z \lambda)|^2 = \sum_{\kappa \kappa'} \tilde{Z}_{\kappa} \frac{e_z(\kappa|q_z \lambda) e_z^*(\kappa'|q_z \lambda)}{v_c \epsilon_0 \sqrt{M_{\kappa} M_{\kappa'}}} \tilde{Z}_{\kappa'}^*. \quad (4)$$

depend on the eigenvalues $\omega(q_z, \lambda)$ and eigenvectors $\vec{e}(\kappa|q_z \lambda)$ of the dynamical matrix $D_{\alpha\beta}(\vec{q}, \kappa)$, which contains all the short and long range interaction between the ionic cores in the insulating state. The eigenvalues $\omega(q_z, \lambda)$ therefore represent the *bare* phonon frequencies in the absence of the charge fluctuations $\delta\rho_n$. The appearance of special q_z -dependent effective charges $\tilde{Z}_{\kappa}(q_z)$ in equ. 4 reflects the different contribution of ions on and between the superconducting layers and is one of the distinctions to the conventional dielectric function. The function $\epsilon_{\text{ph}}^L(q_z, \omega)$ has zeros at the longitudinal eigenfrequencies $\omega(q_z, \lambda)$ of modes with polarization in c -direction.

A similar consideration [7] shows the general form

$$\epsilon_{\text{ph}}(\vec{q}, \omega) = 1 + \frac{\chi(\vec{q}, \omega)}{1 - f(\vec{q})\chi(\vec{q}, \omega)} \quad (5)$$

of the phononic dielectric constant, which reduces in special cases to the longitudinal $\epsilon_{\text{ph}}^L(q_z) = \epsilon_{\text{ph}}(q_{||} = 0, q_z)$ and transversal dielectric constant $\epsilon_{\text{ph}}^T(q_{||}) = \epsilon_{\text{ph}}(q_{||}, q_z = 0) = \epsilon_\infty^T + \chi(q_{||}, \omega)$, which is relevant in optical experiments.

With the knowledge of the phononic dielectric function ϵ_{ph} the $I_{\text{dc}}-V_{\text{dc}}$ -curve can be calculated with the ansatz

$$\gamma_n(t) = \begin{cases} \gamma_0 + \omega t + \delta\gamma_n(t) & n \text{ resistive} \\ \gamma_0 + \delta\gamma_n(t) & n \text{ else} \end{cases}, \quad (6)$$

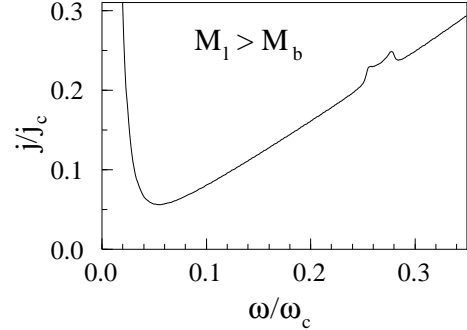


Figure 1. $I_{\text{dc}}-V_{\text{dc}}$ -curve of the first branch in the two-atomic chain model ($M_l > M_b$).

by linearizing in the small oscillating parts $\delta\gamma_n(t) \ll 1$. The final result for the first branch ($V_{\text{dc}} = \hbar\omega/(2e)$, $\omega_p^2 := 2edj_c/(\hbar\epsilon_0)$)

$$j(V) = j_{\text{qp}}(V) - \frac{j_c}{2} \frac{\omega_p^2}{\omega^2} \text{Im} \frac{1}{\tilde{\epsilon}(\omega)} \quad (7)$$

exhibits a phonon resonance *exactly* at the zeros of the modified dielectric function

$$\tilde{\epsilon}(\omega) = \left[\frac{1}{N_z} \sum_{q_z} \frac{1}{\epsilon_{\text{ph}}^L(q_z, \omega) - \frac{\omega_p^2}{\omega^2} + \frac{i\sigma}{\epsilon_0 \omega}} \right]^{-1} + \frac{\omega_p^2}{\omega^2}, \quad (8)$$

i.e. in the unrenormalized phonon bands $\omega(\vec{q}, \lambda)$. More specifically peaks develop at the van-Hove Singularities of the phonon density of states due to the averaging over q_z in equ. 8.

As a reliable microscopic lattice dynamical theory for the dynamical matrix is not yet available and as the intrinsic Josephson effect has to be treated in a phenomenological (one-band) picture until the details of the pairing mechanism are understood, the above results will be illustrated qualitatively in a simple model of a two-atomic chain of masses M_{κ} and charges $Z_1 = -Z_2$.

If the mass on the layer (M_l) is larger than the one in the barrier (M_b), the acoustical van-Hove singularity is suppressed, but the optical band shows a double peak at the band edges (cf. fig. 1), the distance being the bandwidth. The (more realistic) case of $M_l < M_b$ exhibits single peaks

at the upper edges of both acoustical and optical bands and is compared with experiment in fig. 3.

If several junctions are in the resistive state, their dynamics is coherent due to the coupling with phonons, even if no other (e.g. inductive) interaction is present. This is important for the application of short junctions as effective high-frequency devices. Analytical expressions similar to equ. 7 for the second branch can in principle distinguish different phase locked solutions in the I_{dc} - V_{dc} -characteristic [6].

3. COLLECTIVE MODES

The zeros of the real part of the total dielectric function

$$\epsilon_{\text{tot}}(\vec{q}, \omega) = \epsilon_{\text{ph}}(\vec{q}, \omega) - \frac{\omega_p^2(\vec{q})}{\omega^2} + \frac{i\sigma}{\epsilon_0\omega}, \quad (9)$$

define the frequencies $\omega_{\text{el-ph}}(\vec{q}, \omega)$ of the collective modes of the coupled conduction electrons and phonons, where the Josephson plasma frequency is given by (λ_{ab} : coherence length):

$$\omega_p(\vec{q}) = \omega_p^2 \left(1 + \frac{c_0^2 q_\parallel^2 / \omega_p^2}{1 - 2 \frac{\lambda_{ab}^2}{d^2} (\cos(q_z d) - 1)} \right). \quad (10)$$

These modes are different from the bare phonon bands $\omega(\vec{q}, \lambda)$ and can in principle be observed in neutron scattering. In fig. 2 the plasma band $\omega_{\text{pl}}(\vec{q})$ for $q_x \ll q_z$ mixes with the longitudinal acoustical (LA) and optical (LO) phonon modes $\omega(\vec{q}, \lambda)$, which are almost dispersionless on this scale. Note especially that a frequency gap of width $\sqrt{2\omega_{\text{pl}}\Omega}$ appears in the spectrum, which is *formally* (not physically) similar to the polariton dispersion of coupled phonons and photons [7].

4. EXPERIMENTAL RESULTS

Recently the explanation of the subgap resonances in Refs.[2–5] with the phonon coupling mechanism presented here could be well confirmed by Raman measurements on the same samples [3,8] and infrared reflectivity experiments with grazing incidence [9,10] (see table 1). Note that in our theory also Raman-active or silent modes may couple to intrinsic Josephson oscillations for $q_z \neq 0$ and that in contrast to optical

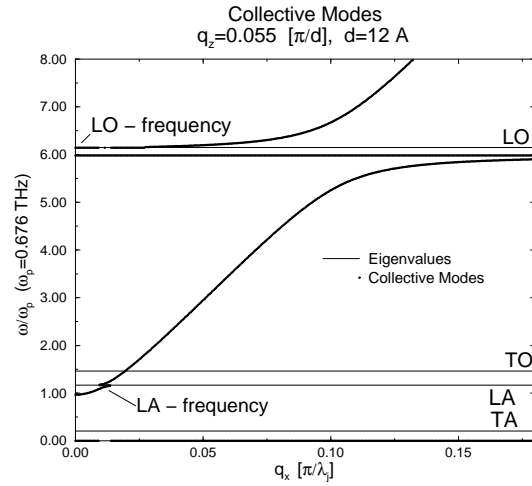


Figure 2. Dispersion $\omega_{\text{el-ph}}(q_x, q_z = 0.055)$ of collective plasma-phonon modes for $q_x \ll q_z$ (horizontal lines: bare phonon frequencies $\omega(\vec{q}, \lambda)$, $\lambda_{ab}/d = 100$, $\lambda_j \approx d\lambda_c/2\lambda_{ab}$).

experiments (at the Γ -point) the whole Brioullin zone contributes in an average way (cf. equ. 8). This provides a reason for slight discrepancies of these experimental data in table 1. For more experimental and theoretical references see [6,9].

The qualitative features of the subgap resonances can already be understood in the local oscillator model of [5]: The position of the resonance is completely independent on temperature, magnetic field or the geometry of the probe, while the intensity of the structure varies $\sim j_c^2$ with the critical current density $j_c(T, B)$. Also the behaviour in external pressure is consistent with the phonon interpretation [8].

Beyond this, in the more general model developed above resonances at van-Hove singularities, e.g. at the upper band edge of the acoustical phonon band, can be described. This might be an explanation for a peak seen in [4] at 3.2 mV ($\hat{=} 1.54$ THz) in the I_{dc} - V_{dc} -characteristic of $\text{Tl}_2\text{Ba}_2\text{Ca}_2\text{Cu}_3\text{O}_{10}$, as the same frequency is predicted in lattice dynamical calculations [11] for the upper edge of the acoustical band and because there are no optical phonon bands at that low fre-

Table 1

Comparison of the frequencies $f_{\text{sg}} = h V_{\text{dc}}/2e$ (in THz) of the most pronounced subgap resonances and of infrared- (f_{LO}) and Raman active (f_{TO}) modes in $\text{Bi}_2\text{Sr}_2\text{CaCu}_2\text{O}_8$ and $\text{Tl}_2\text{Ba}_2\text{Ca}_2\text{Cu}_n\text{O}_{2n+4}$.

Phonons in $\text{Bi}_2\text{Sr}_2\text{CaCu}_2\text{O}_8$				
f_{sg}	2.97	3.89	5.17	5.60
f_{LO}	2.85		5.07	[9]
f_{LO}	2.86		5.16	[10]
f_{TO}		3.80		[3,8]
Phonons in $\text{Tl}_2\text{Ba}_2\text{Ca}_2\text{Cu}_n\text{O}_{2n+4}$				
f_{sg}	3.63	4.64		[5] $n = 3$
f_{LO}		4.50		[9] $n = 2$

quency (cf. Fig. 3). Also the double peaks shown in fig. 1 might have been seen in the satellite structures at 5.17 THz (10.7 mV) and 5.6 (11.6 mV) in the $I_{\text{dc}}-V_{\text{dc}}$ -curve of $\text{Bi}_2\text{Sr}_2\text{CaCu}_2\text{O}_{8+\delta}$ [5], which is consistent with the theoretical width ~ 0.3 THz of this phonon band [11].

5. CONCLUSIONS

In this contribution the microscopic theory for the coupling between Josephson oscillations and longitudinal phonons in intrinsic Josephson systems like the highly anisotropic cuprate superconductors has been developed. The analytical result equ. (7) for the $I_{\text{dc}}-V_{\text{dc}}$ -curve for one resistive junction and the detailed form of the longitudinal dielectric function equ. (2) describing the coupling has been obtained. In particular, not only optical but also acoustical phonons at the edge of the Brillouin zone couple to Josephson oscillations explaining a structure observed in [4] in the $I_{\text{dc}}-V_{\text{dc}}$ -curve occurring at low voltage. The discussion of the dispersion of collective phonon-electron modes is an important first step to understand the effect of phonons in long junctions [7].

The authors thank A. Yurgens, A. Tsvetkov, A. Mayer, D. Strauch, R. Kleiner, P. Müller, L. Bulaevskii and A. Bishop for fruitful discussions and DFG, FORSUPRA and DOE under contract W-7405-ENG-36 (C.H.) for financial support.

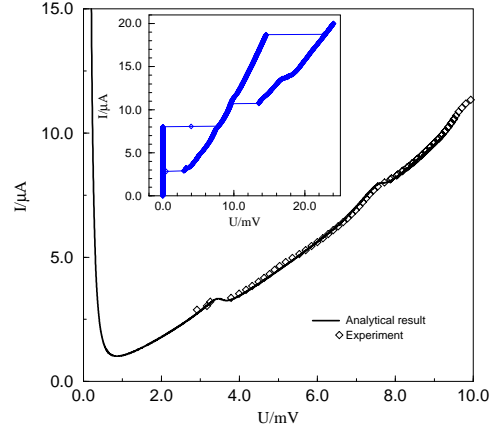


Figure 3. Fit of the experimental $I_{\text{dc}}-V_{\text{dc}}$ -curve in $\text{Tl}_2\text{Ba}_2\text{Ca}_2\text{Cu}_3\text{O}_{10}$ [4] near the band edge of the acoustical branch (at 1.5 THz) and an optical branch within the two-atomic chain model (inset: first two resistive branches).

REFERENCES

1. R. Kleiner et al., Phys. Rev. Lett. **68**, 2394 (1992); R. Kleiner et al., Phys. Rev. B **49** (1994), 1327.
2. K. Schlenga, et al., Phys. Rev. Lett. **76**, 4943 (1996).
3. A. Yurgens et al., Proceedings of SPIE, Vol **2697**, 433 (1996).
4. P. Seidel et al., Physica C **293**, 49 (1997).
5. Ch. Helm et al., Phys. Rev. Lett. **79**, 737 (1997); Ch. Helm et al., Physica C **293**, 60 (1997); K. Schlenga et al., Phys. Rev. B **57**, 14518 (1998).
6. Ch. Helm et al., submitted to Phys. Rev. B, cond-mat/9909318.
7. Ch. Preis, K. Schmalzl, Ch. Helm, J. Keller, in preparation.
8. A. Yurgens, private communication.
9. A. A. Tsvetkov et. al., preprint.
10. S. Tajima et al., Phys. Rev. B **48**, 16164 (1993).
11. A. D. Kulkarni et al., Phys. Rev. B **43**, 5451 (1991).